












ARTICLE

Biallelic variants in the calpain regulatory subunit *CAPNS1* cause pulmonary arterial hypertension



Alex V. Postma^{1,2} , Christina K. Rapp³ , Katrin Knoflach³, Alexander E. Volk⁴, Johannes R. Lemke^{5,6} , Maximilian Ackermann⁷ , Nicolas Regamey⁸, Philipp Latzin⁹, Lucas Celant¹⁰ , Samara M.A. Jansen¹⁰, Harm J. Bogaard¹⁰ , Aho Ilgun², Mariëlle Alders², Karin Y. van Spaendonck-Zwarts², Danny Jonigk¹¹ , Christoph Klein³, Stefan Gräf^{12,13}, Christian Kubisch⁴, Arjan C. Houweling^{2,*} , Matthias Griese^{3,*} 

ARTICLE INFO

Article history:

Received 2 December 2022

Received in revised form

6 April 2023

Accepted 10 April 2023

Available online 23 April 2023

Keywords:

Angiogenesis

Calpain

CAPNS1

Pulmonary arterial hypertension

ABSTRACT

Purpose: The aim of this study was to identify the monogenic cause of pulmonary arterial hypertension (PAH), a multifactorial and often fatal disease, in 2 unrelated consanguine families.

Methods: We performed exome sequencing and validated variant pathogenicity by whole-blood RNA and protein expression analysis in both families. Further RNA sequencing of preserved lung tissue was performed to investigate the consequences on selected genes that are involved in angiogenesis, proliferation, and apoptosis.

Results: We identified 2 rare biallelic variants in *CAPNS1*, encoding the regulatory subunit of calpain. The variants cosegregated with PAH in the families. Both variants lead to loss of function (LoF), which is demonstrated by aberrant splicing resulting in the complete absence of the *CAPNS1* protein in affected patients. No other LoF *CAPNS1* variant was identified in the genome data of more than 1000 patients with unresolved PAH.

Conclusion: The calpain holoenzyme was previously linked to pulmonary vascular development and progression of PAH in patients. We demonstrated that biallelic LoF variants in *CAPNS1* can cause idiopathic PAH by the complete absence of *CAPNS1* protein. Screening of this gene in patients who are affected by PAH, especially with suspected autosomal recessive inheritance, should be considered.

© 2023 The Authors. Published by Elsevier Inc. on behalf of American College of Medical Genetics and Genomics. This is an open access article under the CC BY-NC-ND license (<http://creativecommons.org/licenses/by-nc-nd/4.0/>).

Introduction

Pulmonary arterial hypertension (PAH) is a multifactorial, progressive, and often fatal disease. Elevated pressure in

pulmonary arteries leads to chronic right ventricular stress and dyspnea during exercise and, in later stages of the disease, at rest.^{1,2} Pulmonary vasculature adapts to this increased pressure by remodeling, that is, the 3 layers of the vessels change

The Article Publishing Charge (APC) for this article was paid by Arjan C. Houweling and Matthias Griese.

Alex V. Postma and Christina K. Rapp contributed equally as co-first authors.

Arjan C. Houweling and Matthias Griese contributed equally as co-last authors.

*Correspondence and requests for materials should be addressed to Matthias Griese, Dr. von Haunersches Kinderspital, University of Munich, Lindwurmstraße 4, D-80337 Munich, Germany. *Email address:* Matthias.griese@med.uni-muenchen.de OR Arjan C. Houweling, Department of Human Genetics, Amsterdam University Medical Centre, Meibergdreef 15, 1105AZ Amsterdam, The Netherlands. *Email address:* a.houweling@amsterdamumc.nl

Affiliations are at the end of the document.

doi: <https://doi.org/10.1016/j.gimo.2023.100811>

2949-7744/© 2023 The Authors. Published by Elsevier Inc. on behalf of American College of Medical Genetics and Genomics. This is an open access article under the CC BY-NC-ND license (<http://creativecommons.org/licenses/by-nc-nd/4.0/>).

their composition and increase in size.³ In recent years, significant progress has been made during the exploration of the pathology, genetics, and treatment of PAH.¹ Current vasodilator treatment options reduce pulmonary blood pressure and result in hemodynamic and functional improvement, however, typically without addressing the underlying cause.²

The identification of the monogenic causes of PAH has substantially advanced our pathophysiological knowledge. However, in the majority of patients with PAH, the disease etiology remains unclear. The genetic diagnostic yield in patients with PAH is still low (up to 25%).^{4,5} Pathogenic variants have mostly been identified in genes from the transforming growth factor- β (TGF- β) signaling pathway.⁶⁻⁸ Indeed, in up to 80% of individuals with genetically solved PAH, the pathogenic variant was identified in *BMPR2*.¹ Besides *BMPR2*, about 20 additional genes have been associated with PAH, which also include non-TGF- β pathway genes.^{9,10}

In general, most genes associated with PAH display an autosomal dominant inheritance pattern, with a high variety in the severity and age of onset of the disease, and an incomplete penetrance.⁴ Consequently, the disease often remains undiagnosed in asymptomatic heterozygotes. Recent studies have also uncovered biallelic variants in children with severe, early-onset PAH, in genes that were previously associated with autosomal dominant adult-onset PAH, for example, *ATP13A3*,¹¹ *GDF2*,¹² and *KCNK3*.¹³ This further highlights the heterogeneity and complexity of the genetic components of PAH.

Here, we describe 2 families with autosomal recessive PAH, one of which has been previously published as an unresolved case (family A).¹⁴ In both families, we identified novel, biallelic, loss-of-function (LoF) variants in the *CAPNS1* gene in affected family members. *CAPNS1*, the calpain small subunit 1, encodes the regulatory subunit of the calpain holoenzyme, which is known to be involved in pulmonary vascular development and the progression of PAH.^{15,16} We confirmed that the identified variants cosegregated with the disease and led to the absence of *CAPNS1* protein in affected members of both families.

Materials and Methods

Family A gave their written informed consent to participate in the chILD-EU diagnosis and genetic analysis program.¹⁷ Family B was enrolled at the UMC in Amsterdam, The Netherlands. They provided written consent for research use of their data. Clinical data were retrieved from patient records.

Exome sequencing and linkage analysis

Genomic DNA was isolated from ethylenediaminetetraacetic acid blood using standard methods. Details on the linkage analysis, exome sequencing, and the bioinformatics pipeline and filtering steps are described in [Supplemental Methods](#).

Complementary DNA analysis

Total RNA from peripheral white blood cells was extracted from fresh ethylenediaminetetraacetic acid blood by a standard trizol protocol.

Preparation of cell fractions and lysates

Peripheral blood mononuclear cells (PBMCs) were isolated from heparinized whole blood by standard Ficoll-Paque density gradient technique.

Western blot analysis

CAPNS1 expression was checked by western blot analysis according to standard procedures using the anti-CAPNS1 antibody (ab92333, Abcam) and GAPDH (RDI-TRK5G4-6C5, Research Diagnostics) as a loading control.

Targeted RNA sequencing

RNA material was isolated out of formaldehyde-fixed paraffin-embedded lung tissue using standard methods. Gene expression of 144 target genes was analyzed using NanoString nCounter technology, as previously described.¹⁸ Calculations were performed using nSolver Analysis Software v.4.0, as detailed in [Supplemental Methods](#). Five age-matched children with a history of nonpulmonary cancer or pulmonary disease without architectural distortion (eg, bronchitis) were selected and used as controls in the measurement. All samples were categorized as tumor free based on histologic examination.

Electromagnetic interference microscopy

The formaldehyde-fixed paraffin-embedded samples were deparaffinized, freeze-dried, and mounted on specimen holders with side-adhesive tape and thin copper wires, and they were fixed to the holders as recording electrodes to ensure a high image resolution. They were then sputtered with gold in an argon atmosphere and analyzed using an ESEM XL-30 scanning electron microscope (Philips).

PAH reference cohort screening

The National Institute for Health and Care Research (NIHR) BioResource for Translational Research–Rare Diseases has sequenced the entire genomes of 13,037 individuals diagnosed with 1 of 15 rare diseases and selected relatives, including 1150 individuals recruited to the PAH domain.¹⁹ We filtered this reference population for rare (minor allele frequency <1 in 1000) protein-coding biallelic LoF variants in *CAPNS1*.

Results

Clinical descriptions of affected families

Proband P1 is the first child of family A of Tunisian origin with consanguineous parents (first-degree cousins; [Table 1](#), [Figure 1A](#)). In the first months of life, she had episodes of apnea with cyanosis, and a diagnosis of hypertrophic cardiomyopathy of unknown origin was made at the age of 1 year. She died in Tunisia at the age of 17 months. Postmortem examination was rejected. The clinical and familial history of patient P2 (second child of family A) has been published before.¹⁴ In brief, after preterm birth, she developed neonatal sepsis and respiratory distress syndrome but was discharged home without symptoms 1 week later. From the age of 15 months onward, she had episodes of apnea and cyanosis and was diagnosed with PAH. Chest computed tomography (CT) imaging revealed bilateral diffuse ground-glass opacities, and a lung biopsy identified pulmonary capillary hemangiomatosis with thickened alveolar septae and abnormally proliferating capillaries. Pulmonary artery pressures normalized under Bosentan treatment. At the age of 18 months, severe respiratory infection with fever, rhinitis, and cough destabilized her, and at the age of 29 months, she died at home, presumably from a pulmonary hypertensive crisis. Postmortem assessment of lung parenchyma and vascular architecture revealed a diffuse thickening of alveolar capillaries by an aberrant proliferation around the bronchovascular bundles. The dilated capillary plexuses within the alveolar septa demonstrated evidence of sprouting and intussusceptive angiogenesis ([Figure 2D](#)).

The youngest sister, patient P3, was born after an uneventful pregnancy, and pulmonary arterial tension was closely monitored (brain natriuretic peptide [BNP] < 50 pg/mL). At the age of 6 months, she developed nocturnal seizures, cyanosis, apnea, and a month later first signs of pulmonary hypertension (PH) were confirmed by echocardiography. At this time, no abnormalities of the size of the heart and pulmonary arteries were recognized. In addition, CT imaging identified inhomogeneous consolidations and single nodular opacities. A lung biopsy identified focal enlargement of the pulmonary arterial branches and discrete septal thickening, indicating pulmonary capillary hemangiomatosis. At the age of 21 months, right heart catheterization measured a mean pulmonary arterial pressure of 33 mm Hg (normal mean pulmonary arterial pressure < 20),²⁰ pulmonary vascular resistance of 5 WU (normal pulmonary vascular resistance < 2),²⁰ and pulmonary arterial wedge pressure of 13 mm Hg (normal pulmonary arterial wedge pressure < 12), demonstrating mild PAH. Chest imaging revealed right heart hypertrophy, and echocardiographic investigation in the following months showed mild dilatation of the right heart. Despite intense treatment using increased doses of sildenafil (up to 3 mg/kg/d) and a final additional administration of Inderal (2 mg/kg/d) and close monitoring, she had severe progression of PH and died at the age of 29 months in a PH crisis.

Proband P4 was the first child of a consanguineous family (first-degree cousins) from Dutch origin (family B). He had cardiopulmonary disease and suspected PH. He died at the age of 5 years. At that time, neither the diagnosis of PH was quantitatively assessed nor any genetic analyses were performed. Unfortunately, the medical records were not available for further information.

Patient P5, the brother of P4, was first referred for cardiologic diagnostics at the age of 26 years because of progressive shortness of breath on exertion and tachycardia in the past year. He reported muscle cramps and proximal weakness of the shoulders and upper legs. Elevated levels of creatine kinase were measured repeatedly (up to 1300 U/L). Muscular biopsy, including electron microscopy, revealed mild nonspecific abnormalities with reduced level of type II cells. In addition, he had trouble closing his eyes completely. He smoked approximately 8 cigarettes a day since the age of 16 and quit smoking a year before referral. CT imaging showed centrilobular ground-glass opacities in the lower lobes. Cardiac evaluation revealed atrial flutter. Ultrasound and cardiac magnetic resonance imaging revealed right atrial and ventricular dilation and mild tricuspid insufficiency. The increased mean pulmonary arterial pressure of 39 mm Hg (normal <20)²⁰ and pulmonary vascular resistance of 4.3 WU (normal <2),²⁰ which were identified by right heart catheterization, demonstrated PAH. As consequence, increased right ventricular afterload resulted in elevated BNP levels (NT-proBNP: 541 ng/L; normal <300).²⁰ At the Department of Neurology, severe paralysis of the facial musculature, proximal paresis of the shoulder and extensor hallucis longus, and nasal dysarthria were observed. However, no definitive neurologic diagnosis was established. In addition, subclinical hyperthyroidism was diagnosed (T4: 28 pmol/L, normal: 12–22) with thyroid-stimulating hormone, anti-thyroid peroxidase, antithyroglobulin, and anti-thyroid-stimulating hormone antibodies in normal range. At the age of 34 years, he had a pacemaker implantation because of atrioventricular block. He developed severe right ventricular failure 3 years later. The patient was evaluated to be too sick for lung transplantation and died at the age of 42 years.

Genetic analyses of consanguineous PAH families

Because of parental consanguinity and the presence of PH in 3 of the 4 children in family A, we suspected an autosomal recessive inheritance and initially performed genome-wide linkage analysis with homozygosity mapping, identifying possible linkage to 5 regions with a logarithm of the odds score of 2.23 ([Supplemental Figure 1](#)). The largest of these regions spans around 15 Mb on chromosome 19q and is delimited by the markers rs11668376 and rs759293.

Trio exome analysis in P2 did not reveal any rare variants in genes previously associated with PH⁹ or cardiomyopathy.²¹ In total, 1 rare compound heterozygote and 8 homozygote variants were identified in P2 (listed in

Table 1 Clinical presentation of the probands

Proband	P1	P2	P3	P4	P5
Family	Fam: A II-1	Fam: A II-2	Fam: A II-3	Fam: B II-1	Fam: B II-2
Gender	Female	Female	Female	Male	Male
Origin	Tunisian, consanguine parents (first-degree cousins)			Dutch, consanguine parents (first-degree cousins)	
Genetic variant in <i>CAPNS1</i>	ND	NC_000019.10(GRCh38) :g.36146313G>A (NM_001749.4):c.721+1G>A		NC_000019.10(GRCh38):g.36142298A>G (NM_001749.4):c.210-2A>G	
ACMG interpretation		Pathogenic (Ib): PVS1, PM2, PM4, PP1, PP3		Pathogenic (Ia): PVS1, PS3, PM2, PP1, PP3	
Onset and course of disease					
Neonatal period	Premature birth	Premature birth, neonatal oxygen and mech. assistance for 1 wk	Premature birth, uneventful	ND	Uneventful
Age at disease PAH onset	12 mo	15 mo	6 mo	ND	22 y
Progressive disease course	++	++	++	++	+
Age at death	17 mo	29 mo	30 mo	5 y	42 y
Respiratory findings					
Progressive respiratory insufficiency	+	+	+	Pulmonary disease (no details available)	-
Apnea	++	++	++		+
Cyanosis	++	++	++		+
BAL	ND	Hemosiderin-laden macrophages	ND	ND	ND
Lung CT imaging	ND	Poorly defined pulmonary vasculature. Bilateral diffuse ground glass opacities in right mediobasal lower segment. Impression of nodularity.	Inhomogeneous condensation and single nodular opacities in right posterior upper segment	ND	Centrilobular ground glass opacities in the lower lobes
Lung histology	ND	Pulmonary capillary hemangiomas	Pulmonary capillary hemangiomas	ND	ND
Cardiac/vascular findings					
Chest x-ray	ND	Normal sized heart, no structural cardiac defects, no sign for central pulmonary artery dilation	Right heart hypertrophy	ND	Enlarged heart, vascular redistribution consistent with edema
ECHO	Hypertrophic cardiomyopathy of unknown origin	Right heart hypertrophy, no pericardial effusion	Right heart hypertrophy, mild dilatation of right heart chamber. No abnormality of biventricular systolic function or cardiac valves, no pericardial effusion	ND	Right atrial and ventricular dilation. Implanted cardioverter defibrillator in situ. Mild tricuspid insufficiency, no pericardial effusion, atrial fibrillation

(continued)

Table 1 Continued

Proband	P1	P2	P3	P4	P5
Heart catheterization references: PASP ≤ 35 mm Hg mPAP ≤ 20 mm Hg PVR ≤ 2 WU	ND	PASP: 60-70 mm Hg mPAP: 25 mm Hg PVR of 3 WU	PASP: 65 mm Hg mPAP: 33 mm Hg PVR of 5 WU	ND	mPAP: 39 mm Hg PVR: 4.3 WU
Reference: NT-proBNP ≤ 300 ng/L	ND	NT-proBNP of 2906 ng/L Normalized under treatment	Normal range	ND	NT-proBNP of 541 ng/L Increased under treatment: 4686 ng/L
Additional findings		Opisthotonus	Breath holding spells		Proximal weakness of arms and legs, nasal dysarthria, dysphagia, lagophthalmus; hypothyroidism
Failure to thrive	+	+	+	ND	-

ACMG, American College of Medical Genetics and Genomics; BAL, bronchiolar lavage; BNP, brain natriuretic peptide; CT, computed tomography; ECHO, echocardiography; mPAP, mean pulmonary arterial pressure; ND, no data; PAH, pulmonary arterial hypertension; PASP, pulmonary arterial systolic pressure; PVR, pulmonary vascular resistance; WU, Wood unit.

Supplemental Table 1). Considering the severe disease in more than 1 affected child, only variants identified in both affected children (P2 and P3) were interpreted based on the guidelines of the American College of Medical Genetics and Genomics.²² Subsequent exome sequencing of the affected sister P3 revealed that she shared only 1 rare homozygous variant with P2 and that this homozygous variant was absent in the healthy sister (II-4) (Figure 1A, Family A). This variant is located within the putative linkage region on chromosome 19, in the *CAPNS1* gene, and affects the highly conserved GU-sequence of the donor splice site of coding exon 8 ((NM_001749.4):c.721+1G>A)²³ (Figure 1B, left). The variant was confirmed by Sanger sequencing and segregated with the disease in the family; indeed, the variant was identified heterozygote in both parents and the healthy sibling (Figure 1A). RNA expression analysis in patient P3 showed that the c.721+1G>A variant led to an in-frame skipping of coding exon 8 (r.604_721del, 117 bp) (Figure 1C), resulting in a *CAPNS1* protein missing 39 amino acids, affecting the fourth and fifth EF-hand domain (Figure 1D). Western blot analysis for the *CAPNS1* protein was performed to assess the consequences of the aberrant transcript; *CAPNS1* is ubiquitously expressed,²⁴ among others in blood. The mutant *CAPNS1* protein was overexpressed in HEK-293 cells to demonstrate antibody specificity. Indeed, both the wild-type and shorter mutant *CAPNS1* protein were detectable in HEK-293 cells (Figure 2A, first lane). However, there was no evidence of a shorter *CAPNS1* protein in PBMCs from the unaffected heterozygous parents and the sister (Figure 2A). This indicates that although aberrant messenger RNA is being produced, messenger RNA is not translated into an aberrant *CAPNS1* protein or mutant protein undergoes an early degradation in PBMCs. To further check this hypothesis, we performed a series of in vitro experiments in which we

demonstrated that the aberrant shorter protein is being degraded by the proteasome. Indeed, the aberrant protein showed a strongly detectable band after adding the proteasome blocker MG-132 (Figure 2B).

In patient P5 (Family B), candidate gene analysis for *BMP2* and *SMAD9* was initially performed, which did not reveal any pathogenic variants. Subsequent exome sequencing did not identify pathogenic variants in genes already associated with cardiomyopathy or PH; indeed, only 1 homozygous splicing variant in *CAPNS1* was identified. The (NM_001749.4):c.210-2A>G²³ variant alters the highly conserved AG acceptor splicing site before coding exon 2 (Figure 1B, right). The variant was confirmed by Sanger sequencing and segregated with the disease in the family. In both parents, the variant was heterozygote, whereas the variant was absent from the healthy sibling (Figure 1A). RNA expression analysis identified 2 aberrant *CAPNS1* transcripts in patient P5, one with a loss of coding exon 2, and the other one used a cryptic splice site within coding exon 2 (c.213_214). Normal *CAPNS1* RNA transcripts were not identified. Both aberrant transcripts are predicted to result in frameshift with creation of a premature stop codon (p.(Glu71Profs*40) and p.(Ser70Argfs*51), respectively). This likely leads to the complete absence of *CAPNS1* protein, which was confirmed using western blot analysis in patient P5 (Figure 2B). Although *CAPNS1* was expressed in PBMCs from the blood of healthy controls, it could not be detected in PBMCs from patient P5.

Both variants were absent in more than 120,000 controls (gnomAD).²⁵ Within gnomAD, there are 4 homozygote LoF variants identified in a noncanonical transcript; however, these are curated as low confidence and are likely technical artifacts.²⁵ Both variants identified in our patients were classified as pathogenic (Ib and Ia) according to ACMG

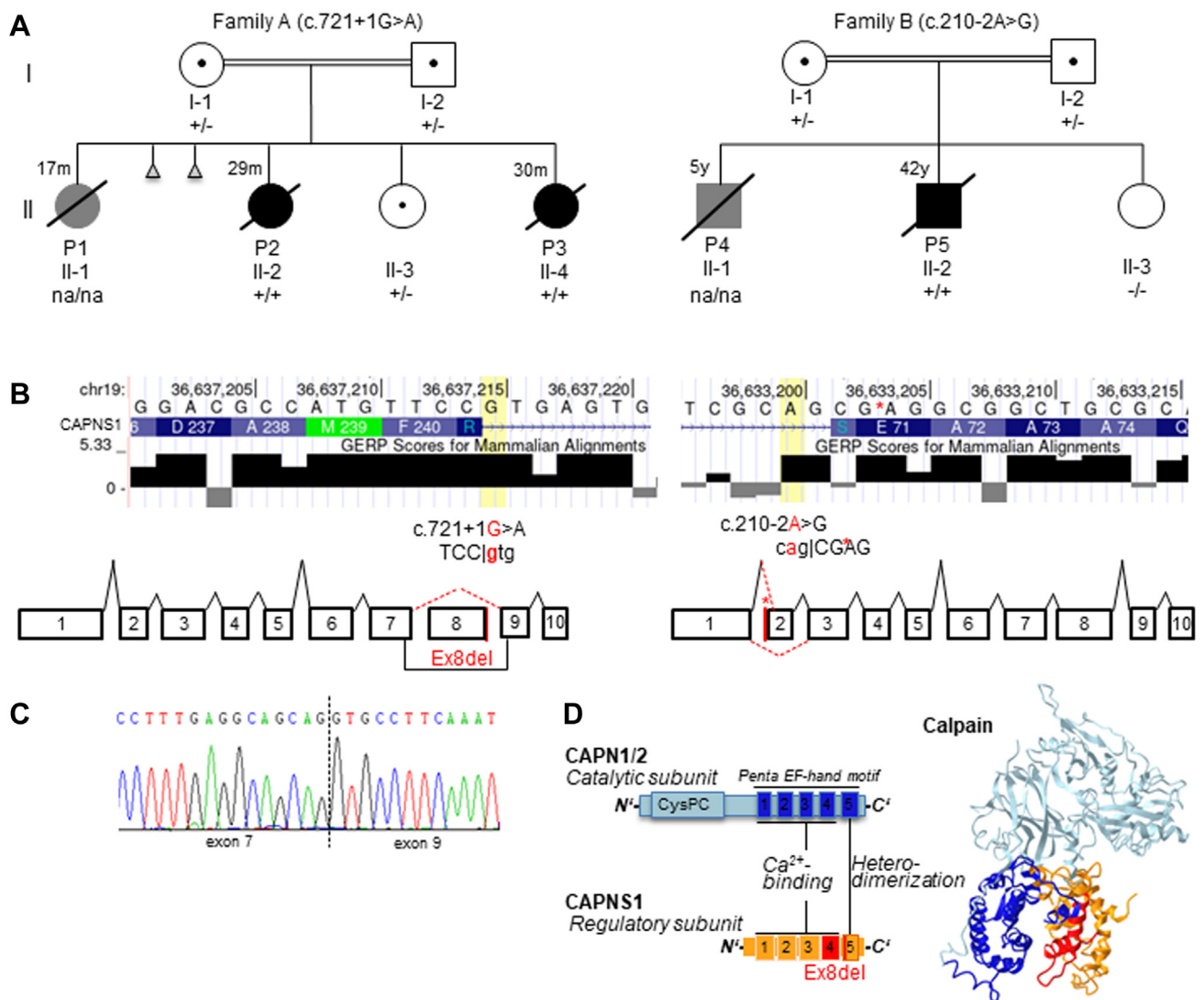


Figure 1 Detailed representation of the biallelic *CAPNS1* variants identified in the probands. A. Schematic drawing of the pedigrees. Clinically affected individuals with confirmed diagnosis of pulmonary alveolar hypertension are depicted in solid black, and individuals with suspected pulmonary hypertension diagnosis are depicted in grey. Healthy individuals are depicted in solid white. Abortion is illustrated as a triangle. Deceased individuals are denoted by a slash, with age of death indicated. Consanguinity is indicated by double lines. +/- variant was identified in homozygote, +/- variant was identified in heterozygote, na/na no genetic information. B. Consequences on splicing of the identified *CAPNS1* variants. The variant identified in family A resulted in skipping of coding exon 8. The variant identified in family B resulted in 2 aberrant transcripts, 1 with skipping of coding exon 2 and 1 using a cryptic splice site within coding exon 2 (between c.213 and c.214), indicating by an asterisk. C. Complementary DNA analysis in patient P3 confirmed the skipping of coding exon 8, without a shift in the reading frame. D. Schematic protein structure. Calpain consists of the catalytic subunit (CAPN1/2: blue) and the regulatory subunit (CAPNS1: orange). Both harbor the penta EF-hand motif, essential for Ca²⁺ binding and heterodimerization. The in-frame deletion of coding exon 8 in family A will potentially result in a CAPNS1 protein lacking the fourth and fifth EF-hand domain (shaded in red). EF, Helix-Loop-Helix; GERP, Genomic Evolutionary Rate Profiling.

guidelines (PVS1, PM2, PM4, PP1, PP3 and PVS1, PS3, PM2, PP1, PP3, respectively).²²

Screening of rare *CAPNS1* variants in reference population

Proband P5 was recruited by the NIHR BioResource for Translational Research–Rare Diseases to participate in the

large-scale sequencing reference population of 13,037 individuals, including 1150 individuals associated to PAH. The sequencing independently confirmed that P5 carried the biallelic *CAPNS1* variant. Apart from proband P5, no biallelic likely pathogenic LoF variants (minor allele frequency < 0.001) were identified in *CAPNS1*, in the 13,037 individuals. This implies that biallelic LoF variants in *CAPNS1* represent a rather rare cause of monogenic PAH.

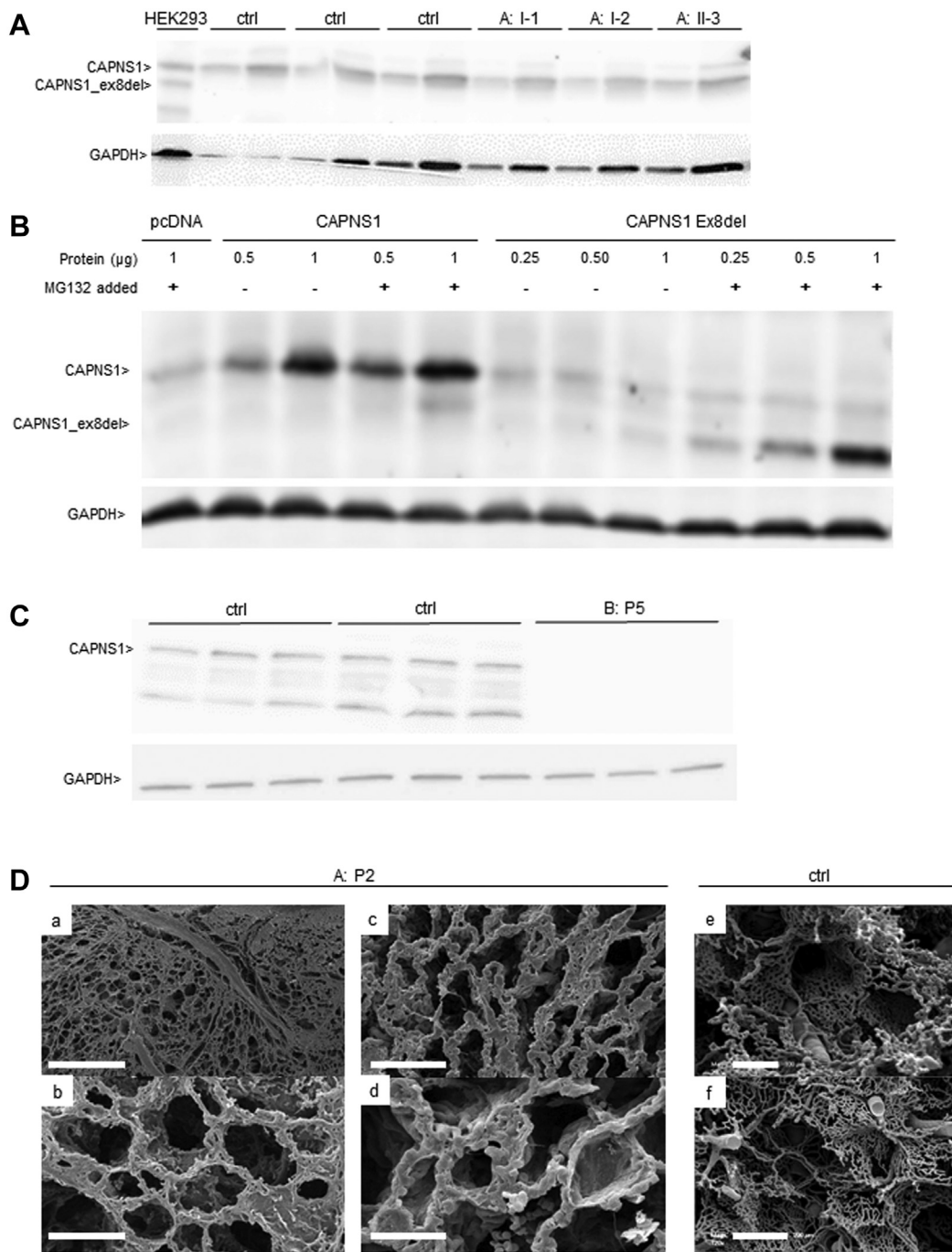


Figure 2 Further analyses in the probands' blood and lung tissue samples. A. CAPNS1 western blot analysis. In all members of family A with identified heterozygote *CAPNS1* variant (c.721+1G>A), no aberrant CAPNS1 protein was detectable compared with HEK cells that overexpressed this CAPNS1 variant (lane 1). All samples demonstrated only 1 band, at the correct height, similar to healthy controls (CAPNS1 = 28 kDa). Of note, GAPDH was used as a loading control (separate blot). B. The aberrant CAPNS1 protein (of the c.721+1G>A variant) was increasingly detectable by adding increasing amounts of the proteasome blocker MG-132. In addition, GAPDH was used as a loading control (separate blot). C. In patient P5, family B, CAPNS1 western blot demonstrates total absence of CAPNS1, in comparison with healthy controls. Furthermore, GAPDH was used as a loading control (separate blot). D. Scanning electron microscopy analysis of lung biopsies. Vascular corrosion casts from patient P2 and a healthy control show a cross-sectional view of the preserved lung parenchyma with (a/b) proliferation around the bronchovascular bundles and (c/d) dilated capillary plexuses within the alveolar septae. (e/f) For comparison, less and small alveolar capillaries in a healthy human lung. Bars: a = 500 μm, b/f = 200 μm, c/e = 100 μm, d = 50 μm. cDNA, complementary DNA; GAPDH, glyceraldehyde 3-phosphate dehydrogenase; HEK, human embryonic kidney.

Targeted RNA sequencing of associated calpain pathways

We performed RNA sequencing from RNA that was isolated from preserved lung material to gain insight into how the identified *CAPNS1* variant affects calpain-mediated pathways and other genes involved in angiogenesis, proliferation, and apoptosis pathways (Supplemental Table 2). The exclusive analysis of just 1 patient (P2, $n = 1$) had no statistical power. Overall changes were small, explorative *t* test analysis pointed out 3 genes of higher interest, illustrated by volcano plot analysis (Figure 3C). The genes *BMP4* (2.87x), *STAT6* (1.97x), and *ACVRL1* (1.80x) showed an increased expression in patient P2 compared with controls (Figure 3D). *CAPNS1* expression was reduced (0.43x). All results are listed in the Supplemental data (Supplemental Table 2).

Discussion

We have identified 2 rare, homozygous variants in the *CAPNS1* gene, encoding the regulatory subunit of the calpain holoenzyme. These variants segregate in 2 unrelated families with idiopathic PH. We demonstrate that these variants lead to absence of the regulatory CAPNS1 protein.

The calpain family is part of a bigger group of calcium activated proteases involved in cell signaling, proliferation, differentiation, and apoptosis.²⁶ Conventional calpains act as holoenzymes by heterodimerization of 1 large catalytic subunit (80 kDa), which is encoded by *CAPN1* or *CAPN2*, and 1 small regulatory subunit (28 kDa), which is encoded by *CAPNS1*. Both, the catalytic and the regulatory subunits have a similar structure of 5 Helix-Loop-Helix (EF)-hand domains, required for calcium binding and heterodimerization (Figure 1D).²⁶ In addition, the regulatory subunit has a suspected chaperone-like function, assumed to be necessary for the conformational changes that are essential for stabilization, calcium-dependent activation, and inhibition by calpastatin.²⁷

We demonstrated that the *CAPNS1* variant in family A resulted in loss of coding exon 8. This exon harbors the fifth EF-hand domain in the regulatory subunit, which is necessary for the interaction with the catalytic subunit, when forming the calpain holoenzyme.^{27,28} Subsequent western blot analysis of family A did not detect an aberrant shorter protein, most likely the result of proteasome-induced degradation. The importance of these EF-hand domains is highlighted by studies in transgenic mice, as one of the knockouts of *Capn4* (the murine homolog to *CAPNS1*)²⁹ was generated with a loss of the C-terminal 38 amino acids representing the fifth EF-hand domain, similar to family A. This disruption of *Capn4* resulted in the total loss of all calpain activity, possibly based on the assumed destabilization of the calpain holoenzyme. These *Capn4*^{-/-} mice were not viable and they died at embryonic day 11.5

because of abnormal vascularization and a cardiac developmental defect.²⁹ The early death limits its further use as a PH disease model, but it does highlight the difference in phenotype and survival between mouse and humans in terms of absent CAPNS1 protein, because homozygous patients in both families A and B were born alive and lived months to years, in the absence of CAPNS1 protein. One possible explanation is that the calpain pathways are differently regulated between these 2 species and that calpain stability and function in humans is retained in absence of the regulatory protein. Such a mechanism could work via alternative homodimerization of 2 catalytic subunits, as seen in other calpain family members (ie, CAPN3).^{30,31}

Despite similar lines, the 2 families presented an apparent degree of variability in the onset and course of disease. It is important to point out that pathogenic variants in PAH-associated genes display a high level of incomplete penetrance, which is likely caused by additional genetic, epigenetic, and/or environmental factors that contribute to disease progression.⁵ Another possible explanation would be the so-called poison-peptide scenario.³² It is well known that the absence of naturally expressed proteins can be recognized by cells, and this, in turn, can lead to expression changes of relevant proteins that can compensate for the loss of the main protein.³³ However, such a compensating mechanism is less efficient or absent in cases in which aberrant proteins are produced. Even though we did not detect a shortened CAPNS1 protein in our experiments in whole blood from family A, it is possible that such a shortened protein is produced in other cells or organs, thereby contributing to the disease. One possible candidate to compensate the CAPNS1 loss could be CAPNS2, a regulatory subunit significantly similar to CAPNS1 and calpain that is able to interact with both regulatory subunits.³⁴ However, because of the large number of 15 calpain isoforms identified to be present in most tissues, our knowledge on the organization and functions of the signaling pathways regulated by these proteases is very limited.²⁶ Taken together, it is as yet unclear why there are phenotypic differences between the 2 families, and future experiments might be able to address this.

In general, we hypothesize that the variations in both affected families lead to an increase in calpain activity because of the loss of the regulatory subunit and the consequent loss of inhibition via calpastatin (Figure 3A and B). This hypothesis was in-line with the observed differences in the expression levels of *ACVRL1* and *BMP4* (Figure 3D) using targeted RNA sequencing in the lung tissue available from patient P2. Both genes play an essential role in the BMP/TGF- β pathway (Figure 3B), which is already known to be associated with the pathogenesis of PAH^{8,10} and in which calpain plays a significant role, that is, by the degradation of SMAD2, an important part of the downstream signaling of TGF- β pathway (Figure 3B). The balance between BMP and TGF- β pathway is crucial for the regulation of vascular remodeling, inflammation, hypertrophy, and fibrosis, especially in the lungs and heart.³⁵ The switch toward *ACVRL1* and *SMAD1/*

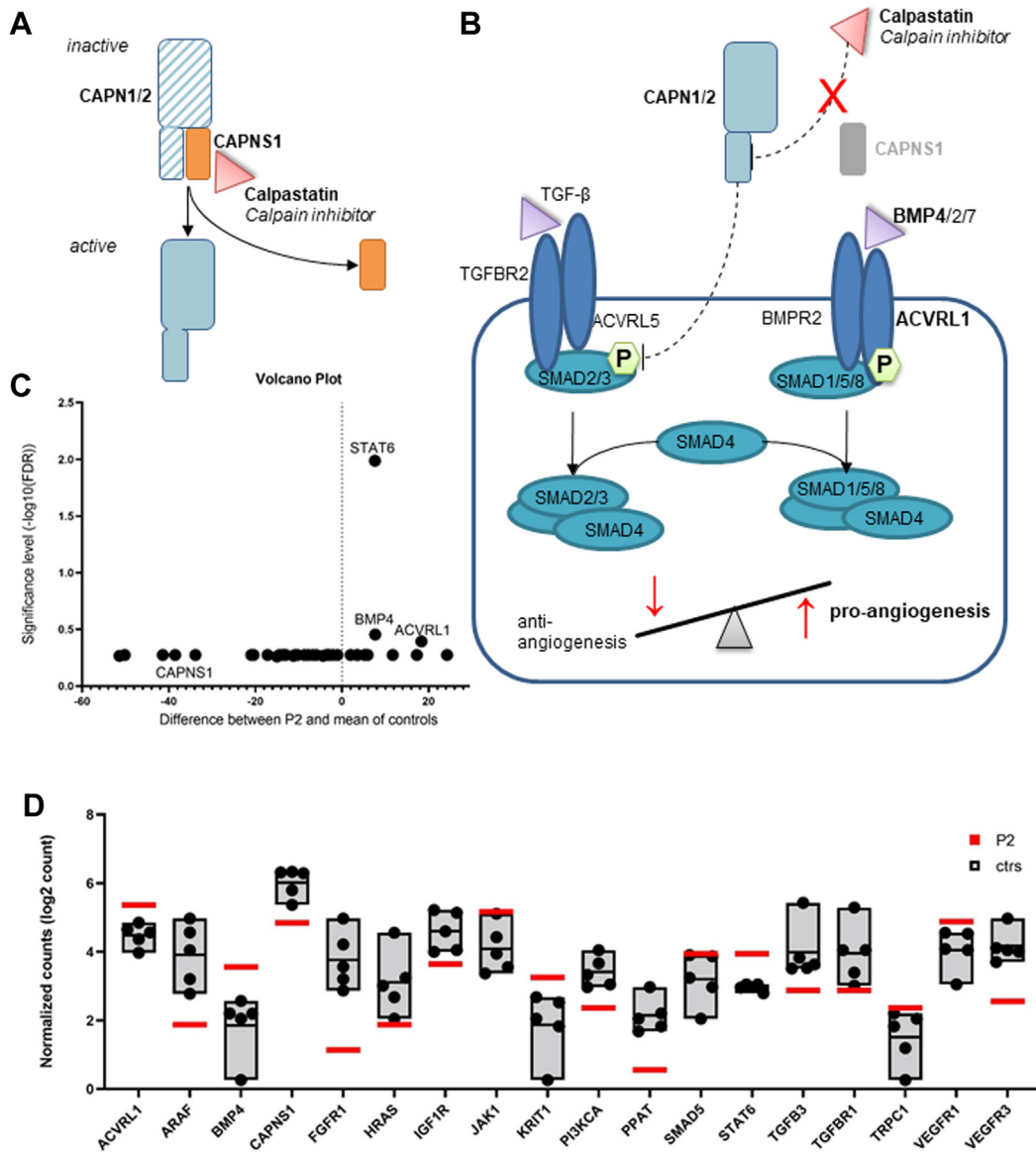


Figure 3 Downstream signaling of calpain in theory and RNA analysis in lung tissue sample of proband P2. A. The calpain holoenzyme is inactive in bound form because of the inhibition via calpastatin. After ubiquitination of CAPNS1 subunit, calpain is active. B. The loss of calpain subunit is assumed to cause a loss of inhibition via calpastatin. Calpain plays a key role in TGF- β pathway by degradation of phosphorylated SMAD2. The TGF- β and BMP pathways build 2 arms of an angiogenesis balance. The loss of calpain regulation is suspected to lead to an unbalanced angiogenesis. C. Multiple *t* test analysis using GraphPad Prism 9.3.1 is illustrated in volcano plot, by plotting the significance (false discovery rate) vs the differences in the counts of RNA molecules. Volcano plot marks the genes of interests of RNA NanoString analysis in patient P2. D. The counts of RNA molecules were normalized, and the gene expression ratio between patient P2 compared with the mean of controls was calculated using nSolver Analysis Software v.4.0. The normalized \log_2 counts of most informative changes in the gene expression are displayed.

5/9, as indicated in our patient P2, could be caused by the increased degradation of *SMAD2* and would consequently promote angiogenesis.³⁵ This is furthermore supported by the fact that the overexpression of *ACVRL1* has been previously described in various animal models with PAH.³⁶ Furthermore, an increase in *BMP4* levels in mice leads to the hemorrhage of capillary endothelial cells in the brain and lung.³⁷ In addition, the targeted RNA sequencing revealed an increased expression in *STAT6*. The degradation

of *STAT6* is directly regulated by the interaction of CAPNS1 with RIP140.³⁸ *STAT6* is involved in the endothelial-to-mesenchymal transition, inflammation, and cytokine recruitment. Hence, the loss of CAPNS1 may result in an increased *STAT6* expression with a consequently increased polarization of M2 macrophages, promoting further angiogenesis and tissue remodeling.

Taken together, we propose that the loss of the regulatory calpain subunit might, in turn, promote proangiogenesis

factors. This would be consistent with the observed aberrant angiogenesis in lung tissue from patient P2 that was characterized as sprouting and intussusceptive angiogenesis. The latter in particular is a rapid process of intravascular septation that produces 2 individual lumens from a single vessel within minutes to hours.³⁹ This rapid form of vascular expansion can lead to early death by right heart ventricular failure,³⁹ which has been demonstrated in the clinical course of all affected subjects in family A, who all died before the age of 2. In addition, previous studies identified one other Mendelian human disease with a gain-of-calpain function: neovascular inflammatory vitreoretinopathy (#MIM 193235). It is associated with heterozygous *CAPN5* variants, which are nonclassical calpain proteases that act independently without a regulatory subunit.⁴⁰ This demonstrates that aberrant calpain function can cause aberrant vascularization.

In conclusion, we propose that proper calpain activity is necessary for normal development of the pulmonary vessels. Aberrant calpain activity caused by the absence of *CAPNS1* in our patients will lead to abnormal pulmonary vessels characterized by sprouting and intussusceptive angiogenesis, and eventually contribute to PAH. Although we observed some hints from the RNA expression analysis, the precise mechanism by which the absence of *CAPNS1* leads to disturbed angiogenesis and disease is subject of further study. Nevertheless, to our knowledge, our data highlight, for the first time in humans, the involvement of the *CAPNS1* gene in the development of PAH. We further demonstrate that PAH can be caused by rare biallelic LoF variants in *CAPNS1* and propose that the screening of this gene should be considered in patients affected by PAH, especially in those with a suspected autosomal recessive inheritance.

Data Availability

The data that support the findings of this study are available from the corresponding author, Matthias Griese, upon reasonable request. The data will be shared upon signing a data transfer agreement between our institutes and the requester. Care will be taken to protect identifiable patient information.

Acknowledgments

The authors thank all probands and families for their kind contribution and participation in the study. The authors also thank NIHR BioResource volunteers for their participation and gratefully acknowledge NIHR BioResource centers, National Health Service (NHS) Trusts, and staff for their contribution and thank the National Institute for Health and Care Research, NHS Blood and Transplant, and Health Data Research UK as part of the Digital Innovation Hub Programme. The views expressed are those of the author(s) and not necessarily those of the NHS, the NIHR, or the

Department of Health and Social Care. Finally, the authors thank GeneMatcher for this cooperation by linking our 2 groups with the interest in the same gene.⁴¹

Funding

This work was supported by chILD-EU (FP7, No. 305653) and the DFG Gr 970/9-1 and 9-2 grants to M.G. and in part supported by the Dutch Cardiovascular Alliance (Grant CVON2017-4: DOLPHIN-GENESIS).

Author Information

Conceptualization: C.K.R., M.G., A.V.P., A.C.H.; Data Curation: C.K.R., A.V.P., C.Ku., C.Kl., A.E.V., M.A., S.G.; Funding Acquisition: M.G., A.C.H.; Investigation: N.R., P.L., C.Ku., K.K., H.J.B., K.Y.v.S.-Z.; Methodology: C.K.R., A.V.P., M.A., D.J.; Project Administration: C.K.R., M.G.; Visualization: C.K.R., A.V.P.; Writing-original draft: C.K.R., M.G.; Writing-review and editing: all authors

Ethics Declaration

For family A, the study was approved by the Ethics Committee of the University of Munich (EK23-5-2011, EK111-13, EK20-329), Germany. For family B, the study was approved by the Ethics Committee of the Amsterdam UMC (W22_441).

ORCIDiS

Alex V. Postma: <http://orcid.org/0000-0003-4874-2487>
 Christina K. Rapp: <http://orcid.org/0000-0002-7371-8158>
 Johannes R. Lemke: <http://orcid.org/0000-0002-4435-6610>
 Maximilian Ackermann: <http://orcid.org/0000-0001-9996-2477>
 Lucas Celant: <http://orcid.org/0000-0001-6727-7539>
 Harm J. Bogaard: <http://orcid.org/0000-0001-5371-0346>
 Danny Jonigk: <http://orcid.org/0000-0002-5251-2281>
 Arjan C. Houweling: <http://orcid.org/0000-0002-7728-7535>
 Matthias Griese: <https://orcid.org/0000-0003-0113-912X>

Conflict of Interest

The authors declare no conflicts of interest.

Additional Information

The online version of this article (<https://doi.org/10.1016/j.gimo.2023.100811>) contains supplementary material, which is available to authorized users.

Affiliations

¹Department of Medical Biology, Amsterdam University Medical Centre, Amsterdam, The Netherlands; ²Department of Human Genetics, Amsterdam University Medical Centre, Amsterdam, The Netherlands; ³Department of Pediatrics, Dr. von Hauner Children's Hospital, LMU Klinikum, Ludwig Maximilians University of Munich, German Center for Lung Research (DZL), Munich, Germany; ⁴Institute of Human Genetics, University Medical Center Hamburg-Eppendorf, Hamburg, Germany; ⁵Institute of Human Genetics, Leipzig University Medical Center, Leipzig, Germany; ⁶Center for Rare Diseases, Leipzig University Medical Center, Leipzig, Germany; ⁷Institute of Functional and Clinical Anatomy, University Medical Centre, Johannes Gutenberg University Mainz, Mainz, Germany; ⁸Division of Paediatric Pulmonology, Children's Hospital, Lucerne Cantonal Hospital, Lucerne, Switzerland; ⁹Division of Paediatric Respiratory Medicine and Allergology, Department of Pediatrics, Inselspital, University Hospital, University of Bern, Bern, Switzerland; ¹⁰Department of Pulmonary Medicine, Amsterdam University Medical Centre, Amsterdam, The Netherlands; ¹¹Institute of Pathology, Medizinische Hochschule Hannover, Hanover, Germany; ¹²Department of Medicine, University of Cambridge, Heart and Lung Research Institute, Cambridge, United Kingdom; ¹³NIHR BioResource for Translational Research–Rare Diseases, University of Cambridge, Cambridge Biomedical Campus, Cambridge, United Kingdom

References

- Hassoun PM. Pulmonary arterial hypertension. *N Engl J Med*. 2021;385(25):2361–2376. <http://doi.org/10.1056/NEJMra2000348>
- Thenappan T, Ormiston ML, Ryan JJ, Archer SL. Pulmonary arterial hypertension: pathogenesis and clinical management. *BMJ*. 2018;360:j5492. <http://doi.org/10.1136/bmj.j5492>
- Tuder RM, Ponticos M, Holmes A. Pathogenesis of pulmonary arterial hypertension. In: Varga J, Denton C, Wigley F, Allano Y, Kuwana M, eds. *Scleroderma: From Pathogenesis to Comprehensive Management*. Springer International Publishing; 2017:385–401.
- Chew JD, Loyd JE, Austin ED. Genetics of pulmonary arterial hypertension. *Semin Respir Crit Care Med*. 2017;38(5):585–595. <http://doi.org/10.1055/s-0037-1606201>
- Morrell NW, Aldred MA, Chung WK, et al. Genetics and genomics of pulmonary arterial hypertension. *Eur Respir J*. 2019;53(1):1801899. <http://doi.org/10.1183/13993003.01899-2018>
- Chida A, Shintani M, Nakayama T, et al. Missense mutations of the BMPR1B (ALK6) gene in childhood idiopathic pulmonary arterial hypertension. *Circ J*. 2012;76(6):1501–1508. <http://doi.org/10.1253/circj.cj-11-1281>
- Ma L, Chung WK. The genetic basis of pulmonary arterial hypertension. *Hum Genet*. 2014;133(5):471–479. <http://doi.org/10.1007/s00439-014-1419-3>
- Nasim MT, Ogo T, Ahmed M, et al. Molecular genetic characterization of SMAD signaling molecules in pulmonary arterial hypertension. *Hum Mutat*. 2011;32(12):1385–1389. <http://doi.org/10.1002/humu.21605>
- Eichstaedt CA, Saßmannshausen Z, Shaikat M, et al. Gene panel diagnostics reveals new pathogenic variants in pulmonary arterial hypertension. *Respir Res*. 2022;23(1):74. <http://doi.org/10.1186/s12931-022-01987-x>
- Fazal S, Bissierier M, Hadri L. Molecular and genetic profiling for precision medicines in pulmonary arterial hypertension. *Cells*. 2021;10(3):638. <http://doi.org/10.3390/cells10030638>
- Machado RD, Welch CL, Haimel M, et al. Biallelic variants of ATP13A3 cause dose-dependent childhood-onset pulmonary arterial hypertension characterised by extreme morbidity and mortality. *J Med Genet*. 2022;59(9):906–911. <http://doi.org/10.1136/jmedgenet-2021-107831>
- Hodgson J, Ruiz-Llorente L, McDonald J, et al. Homozygous GDF2 nonsense mutations result in a loss of circulating BMP9 and BMP10 and are associated with either PAH or an “HHT-like” syndrome in children. *Mol Genet Genomic Med*. 2021;9(12):e1685. <http://doi.org/10.1002/mgg3.1685>
- Navas Tejedor P, Tenorio Castaño J, Palomino Doza J, et al. An homozygous mutation in KCNK3 is associated with an aggressive form of hereditary pulmonary arterial hypertension. *Clin Genet*. 2017;91(3):453–457. <http://doi.org/10.1111/cge.12869>
- Navarini S, Bucher B, Pavlovic M, et al. Pulmonary hypertension presenting with apnea, cyanosis, and failure to thrive in a young child. *Chest*. 2011;140(4):1086–1089. <http://doi.org/10.1378/chest.10-2607>
- Barr FE. Calpain: a new target in pulmonary hypertension? *Crit Care Med*. 2005;33(3):693. <http://doi.org/10.1097/01.ccm.0000155913.35077.db>
- Kovacs L, Han W, Rafikov R, et al. Activation of calpain-2 by mediators in pulmonary vascular remodeling of pulmonary arterial hypertension. *Am J Respir Cell Mol Biol*. 2016;54(3):384–393. <http://doi.org/10.1165/rcmb.2015-0151OC>
- Griese M, Seidl E, Hengst M, et al. International management platform for children's interstitial lung disease (chILD-EU). *Thorax*. 2018;73(3):231–239. <http://doi.org/10.1136/thoraxjnl-2017-210519>
- Ackermann M, Verleden SE, Kuehnel M, et al. Pulmonary vascular endothelialitis, thrombosis, and angiogenesis in Covid-19. *N Engl J Med*. 2020;383(2):120–128. <http://doi.org/10.1056/NEJMoa2015432>
- Gräf S, Haimel M, Bleda M, et al. Identification of rare sequence variation underlying heritable pulmonary arterial hypertension. *Nat Commun*. 2018;9(1):1416. <http://doi.org/10.1038/s41467-018-03672-4>
- Humbert M, Kovacs G, Hoeper MM, et al. 2022 ESC/ERS Guidelines for the diagnosis and treatment of pulmonary hypertension. *Eur Heart J*. 2022;43(38):3618–3731. <http://doi.org/10.1093/eurheartj/ehac237>
- Fernlund E, Kissopoulou A, Green H, et al. Hereditary hypertrophic cardiomyopathy in children and young adults—the value of reevaluating and expanding gene panel analyses. *Genes (Basel)*. 2020;11(12):1472. <http://doi.org/10.3390/genes11121472>
- Richards CS, Bale S, Bellissimo DB, et al. ACMG recommendations for standards for interpretation and reporting of sequence variations: revisions 2007. *Genet Med*. 2008;10(4):294–300. <http://doi.org/10.1097/GIM.0b013e31816b5cae>
- Freeman PJ, Hart RK, Gretton LJ, Brookes AJ, Dagleish R. VariantValidator: accurate validation, mapping, and formatting of sequence variation descriptions. *Hum Mutat*. 2018;39(1):61–68. <http://doi.org/10.1002/humu.23348>
- Carithers LJ, Ardlie K, Barcus M, et al. A novel approach to high-quality postmortem tissue procurement: the GTEx project. *Biopreserv Biobank*. 2015;13(5):311–319. <http://doi.org/10.1089/bio.2015.0032>
- Karczewski KJ, Francioli LC, Tiao G, et al. The mutational constraint spectrum quantified from variation in 141,456 humans. *Nature*. 2020;581(7809):434–443. <http://doi.org/10.1038/s41586-020-2308-7>
- Goll DE, Thompson VF, Li H, Wei W, Cong J. The calpain system. *Physiol Rev*. 2003;83(3):731–801. <http://doi.org/10.1152/physrev.00029.2002>
- Suzuki K, Hata S, Kawabata Y, Sorimachi H. Structure, activation, and biology of calpain. *Diabetes*. 2004;53(suppl 1):S12–S18. <http://doi.org/10.2337/diabetes.53.2007.s12>

28. Sorimachi H, Hata S, Ono Y. Calpain chronicle—an enzyme family under multidisciplinary characterization. *Proc Jpn Acad Ser B Phys Biol Sci.* 2011;87(6):287-327. <http://doi.org/10.2183/pjab.87.287>
29. Arthur JS, Elce JS, Hegadorn C, Williams K, Greer PA. Disruption of the murine calpain small subunit gene, *Capn4*: calpain is essential for embryonic development but not for cell growth and division. *Mol Cell Biol.* 2000;20(12):4474-4481. <http://doi.org/10.1128/MCB.20.12.4474-4481.2000>
30. Ravulapalli R, Campbell RL, Gauthier SY, Dhe-Paganon S, Davies PL. Distinguishing between calpain heterodimerization and homodimerization. *FEBS J.* 2009;276(4):973-982. <http://doi.org/10.1111/j.1742-4658.2008.06833.x>
31. Ravulapalli R, Diaz BG, Campbell RL, Davies PL. Homodimerization of calpain 3 penta-EF-hand domain. *Biochem J.* 2005;388(2):585-591. <http://doi.org/10.1042/BJ20041821>
32. Marian AJ, Roberts R. The molecular genetic basis for hypertrophic cardiomyopathy. *J Mol Cell Cardiol.* 2001;33(4):655-670. <http://doi.org/10.1006/jmcc.2001.1340>
33. Parts L, Batté A, Lopes M, et al. Natural variants suppress mutations in hundreds of essential genes. *Mol Syst Biol.* 2021;17(5):e10138. <http://doi.org/10.15252/msb.202010138>
34. Curcio M, Salazar IL, Mele M, Canzoniero LM, Duarte CB. Calpains and neuronal damage in the ischemic brain: the swiss knife in synaptic injury. *Prog Neurobiol.* 2016;143:1-35. <http://doi.org/10.1016/j.pneurobio.2016.06.001>
35. Rol N, Kurakula KB, Happé C, Bogaard HJ, Goumans MJ. TGF-beta and BMPR2 signaling in PAH: two black sheep in one family. *Int J Mol Sci.* 2018;19(9):2585. <http://doi.org/10.3390/ijms19092585>
36. Gore B, Izikki M, Mercier O, et al. Key role of the endothelial TGF-beta/ALK1/endoglin signaling pathway in humans and rodents pulmonary hypertension. *PLoS One.* 2014;9(6):e100310. <http://doi.org/10.1371/journal.pone.0100310>
37. Kiyono M, Shibuya M. Inhibitory Smad transcription factors protect arterial endothelial cells from apoptosis induced by BMP4. *Oncogene.* 2006;25(54):7131-7137. <http://doi.org/10.1038/sj.onc.1209700>
38. Lin YW, Lee B, Liu PS, Wei LN. Receptor-interacting Protein 140 orchestrates the dynamics of macrophage M1/M2 polarization. *J Innate Immun.* 2016;8(1):97-107. <http://doi.org/10.1159/000433539>
39. Ackermann M, Mentzer SJ, Kolb M, Jonigk D. Inflammation and intussusceptive angiogenesis in COVID-19: everything in and out of flow. *Eur Respir J.* 2020;56(5):2003147. <http://doi.org/10.1183/13993003.03147-2020>
40. Mahajan VB, Skeie JM, Bassuk AG, et al. Calpain-5 mutations cause autoimmune uveitis, retinal neovascularization, and photoreceptor degeneration. *PLoS Genet.* 2012;8(10):e1003001. <http://doi.org/10.1371/journal.pgen.1003001>
41. Sobreira N, et al. GeneMatcher: a matching tool for connecting investigators with an interest in the same gene. *Hum Mutat.* 2015;36(10):928-930. <http://doi.org/10.1002/humu.22844>